

## FOREWORD

This work was conducted by the National Carbon Company, a Division of Union Carbide Corporation, under USAF Contract AF 33(616)-6915. This contract was initiated under Project No. 7350 "Refractory Inorganic Non-Metallic Materials", Task No. 735002 "Refractory Inorganic Non-Metallic Materials: Graphitic"; Project No. 7381 "Materials Application", Task No. 738102 "Materials Process"; and Project No. 7-817 "Process Development for Graphite Materials". The work was administered under the direction of the AF Materials Laboratory, Aeronautical Systems Division, with Captain R. H. Wilson, L. J. Conlon and W. P. Conrardy acting as Project Engineers.

Work under this contract has been in progress since May 1, 1960. The work covered in this report was conducted at the Research Laboratory of the National Carbon Company located at Parma 30, Ohio, under the direction of J. C. Bowman, Director of Research and W. P. Eatherly, Assistant Director of Research.

Other reports issued under USAF Contract AF 33(616)-6915 have included:

WADD Technical Notes 61-18 and 61-18, Part II, progress reports covering work from the start of the Contract on May 1, 1960 to October 15, 1961, and the following volumes of WADD Technical Report 61-72 covering various subject phases of the work:

- Volume I Observations by Electron Microscopy of Dislocations in Graphite, by R. Sprague.
- Volume II Applications of Anisotropic Elastic Continuum Theory to Dislocations in Graphite, by G. B. Spence.
- Volume III Decoration of Dislocations and Low Angle Grain Boundaries in Graphite Single Crystals, by R. Bacon and R. Sprague.
- Volume IV Adaptation of Radiographic Principles to the Quality Control of Graphite, by R. W. Wallouch.
- Volume V Analysis of Creep and Recovery Curves for ATJ Graphite, by E. J. Seldin and R. N. Draper.
- Volume VI Creep of Carbons and Graphites in Flexure at High Temperatures, by E. J. Seldin.
- Volume VII High Density Recrystallized Graphite by Hot Forming, by E. A. Neel, A. A. Kellar and K. J. Zeitsch.
- Volume VII High Density Recrystallized Graphite by Hot Forming, Suppl. by G. L. Rowe and M. B. Carter.

# Contrails

- Volume VIII Electron Spin Resonance in Polycrystalline Graphite, by L. S. Singer and G. Wagoner.
- Volume IX Fabrication and Properties of Carbonized Cloth Composites, by W. C. Beasley and E. L. Piper.
- Volume X Thermal Reactivity of Aromatic Hydrocarbons, by I. C. Lewis and T. Edstrom.
- Volume X Suppl. Thermal Reactivity of Aromatic Hydrocarbons, by I. C. Lewis and T. Edstrom.
- Volume XI Characterization of Binders Used in the Fabrication of Graphite Bodies, by E. de Ruiter, A. Halleux, V. Sandor and H. Tschamler.
- Volume XI Suppl. Characterization of Binders Used in the Fabrication of Graphite Bodies, E. de Ruiter, J. F. M. Oth, V. Sandor and H. Tschamler.
- Volume XII Development of an Improved Large Diameter Fine Grain Graphite for Aerospace Applications, by C. W. Waters and E. L. Piper.
- Volume XII Suppl. Development of an Improved Large Diameter Fine Grain Graphite for Aerospace Applications, by R. L. Racicot and C. W. Waters.
- Volume XIII Development of a Fine-Grain Isotropic Graphite for Structural and Substrate Applications, by R. A. Howard and E. L. Piper.
- Volume XIII Suppl. Development of a Fine-Grain Isotropic Graphite for Structural and Substrate Applications, by R. A. Howard and R. L. Racicot.
- Volume XIV Study of High Temperature Tensile Properties of ZTA Grade Graphite, by R. M. Hale and W. M. Fassell, Jr.
- Volume XV Alumina-Condensed Furfuryl Alcohol Resins, by C. W. Boquist, E. R. Nielsen, H. J. O'Neil and R. E. Patcher.
- Volume XVI An Electron Spin Resonance Study of Thermal Reactions of Organic Compounds, by L. S. Singer and I. C. Lewis.
- Volume XVII Radiography of Carbon and Graphite, by T. C. Furnas, Jr. and M. R. Rosumny.
- Volume XVIII High Temperature Tensile Creep of Graphite, by E. J. Seldin.
- Volume XIX Thermal Stresses in Anisotropic Hollow Cylinders, by Tu-Lung Weng.

# Contrails

- Volume XX The Electric and Magnetic Properties of Pyrolytic Graphite, by G. Wagoner and B. H. Eckstein.
- Volume XXI Arc Image Furnace Studies of Graphite, by M. R. Null and W. W. Lozier.
- Volume XXII Photomicrographic Techniques for Carbon and Graphite, by G. L. Peters and H. D. Shade.
- Volume XXIII A Method for Determining Young's Modulus of Graphite at Elevated Temperatures, by S. O. Johnson and R. B. Dull.
- Volume XXIV The Thermal Expansion of Graphite in the c-Direction, by C. E. Lowell.
- Volume XXV Lamellar Compounds of Nongraphitized Petroleum Cokes, by H. F. Volk.
- Volume XXVI Physical Properties of Some Newly Developed Graphite Grades, by R. B. Dull.

# *Contrails*

## ABSTRACT

The variation of graphite properties with chemical structure is illustrated for synthetic graphites prepared from 35 pure aromatic compounds. Detailed chemical and physical studies have been directed to the carbonization of two model aromatic hydrocarbons, acenaphthylene and 9,9'-bifluorenyl. These compounds exhibit extremes in graphitization behavior and the chemical reaction mechanisms are found to be consistent with the nature of the final graphitic products.

Carbonization studies have been extended to the effects of aromatic quinone additives on the carbonization behavior of polynuclear aromatic hydrocarbons. Quinones are shown to effect a general increase in coking value of the polynuclear aromatics and of complex aromatic mixtures. The mechanisms of these interactions are discussed.

This technical documentary report has been reviewed and is approved.



W. G. RAMKE  
Chief, Ceramics and Graphite Branch  
Metals and Ceramics Division  
AF Materials Laboratory

TABLE OF CONTENTS

	<u>PAGE</u>
1. INTRODUCTION . . . . .	1
2. CHEMICAL STRUCTURE AND GRAPHITIZATION . . . . .	2
3. CARBONIZATION OF ACENAPHTHYLENE . . . . .	4
3.1. General Properties of Acenaphthylene (C <sub>12</sub> H <sub>8</sub> ) . . . . .	4
3.2. Differential Thermal Analysis (DTA) . . . . .	4
3.3. Thermogravimetric Analysis (TGA) . . . . .	4
3.4. Volatile Products of Acenaphthylene Pyrolysis . . . . .	4
3.5. Pyrolytic Studies on Acenaphthylene . . . . .	6
3.6. Ultraviolet Spectra of Acenaphthylene Thermal Residues . . . . .	6
3.7. Infrared Spectra of Acenaphthylene Thermal Residues . . . . .	6
3.8. Carbonization Mechanism of Acenaphthylene . . . . .	6
4. CARBONIZATION OF 9, 9'-BIFLUORENYL . . . . .	13
4.1. General Properties of 9, 9'-Bifluorenyl . . . . .	13
4.2. Differential Thermal Analysis . . . . .	13
4.3. Thermogravimetric Analysis (TGA) . . . . .	14
4.4. Pyrolytic Studies on 9, 9'-Bifluorenyl . . . . .	14
4.5. Ultraviolet Absorption Spectra of Bifluorenyl Thermal Residues . . . . .	14
4.6. Infrared Spectra of Bifluorenyl Thermal Residues . . . . .	15
4.7. Thermal Reactions for 9, 9'-Bifluorenyl . . . . .	17
5. THE EFFECTS OF QUINONE ADDITIVES ON THE CARBONIZATION OF POLYNUCLEAR AROMATICS . . . . .	19
5.1. Mechanisms of Quinone-Aromatic Interactions . . . . .	19

# Contrails

	<u>PAGE</u>
5.2. Experimental . . . . .	20
5.3. Results and Discussion . . . . .	20
6. REFERENCES . . . . .	27

LIST OF ILLUSTRATIONS

<u>FIGURE</u>		<u>PAGE</u>
1.	DTA and TGA Thermograms of Acenaphthylene . . . . .	5
2.	UV Spectra of Heat-Treated Acenaphthylene . . . . .	7
3.	IR Spectra of Heat-Treated Acenaphthylene . . . . .	8
4.	UV Spectra of Acenaphthylene Pyrolysis Products . . . . .	9
5.	DTA and TGA Thermograms of 9, 9'-Bifluorenyl and 9, 9'-Bifluorylidene . . . . .	13
6.	UV Spectra of Heat-Treated 9, 9'-Bifluorenyl . . . . .	15
7.	Infrared Spectra of Heat-Treated 9, 9'-Bifluorenyl . . . . .	16
8.	Infrared and Ultraviolet Spectra of Tetrabenzonaphthalene . . . . .	18



LIST OF TABLES

<u>TABLE</u>		<u>PAGE</u>
1.	X-Ray Comparison of Synthetic Graphite from Aromatic Compounds . . . . .	3
2.	Major Volatiles from Thermal Reaction of Acenaphthylene, 25 - 600°C . . . . .	5
3.	Properties of Acenaphthylene Heat-Treated Series . . . . .	7
4.	Chemical Data for 9, 9'-Bifluorenyl Heat-Treated Series. . . . .	14
5.	Effect of Quinones on the Coking Values of Acenaphthene. . . . .	21
6.	Coking Interaction of p-Benzoquinone with Aromatic Hydrocarbons . . . . .	22
7.	Coking Interactions of p-Benzoquinone with Aromatic Hydrocarbons Containing Aliphatic Hydrogens in the Ring . . . . .	24
8.	Coking Values of Pure Materials Employed in Quinone Pitch Study . . . . .	24
9.	Effects of Quinone Additives on Coking Values of Coal Tar Pitches . . . . .	25

# *Contrails*

## 1. INTRODUCTION

The role of chemical composition on the carbonization reactivity of raw materials for carbon and graphite has been discussed previously<sup>(1)</sup>. In this manner it has been shown that the thermal reactivity of carbon precursors is dependent to a large extent on chemical structure. The major interest in understanding the relationships between raw materials and graphite must include not only the effects of chemical structure on the degree of thermal reactivity but also on the course of thermal reaction.

The present report will show that chemical structure can decidedly influence the graphitization sequence and thus the ultimate kind of graphite obtained. This conclusion will be further established from the results obtained from our continuing detailed study of the pyrolysis of two pure aromatic hydrocarbons. Our current views of reaction mechanisms are discussed. Additionally, this report describes the thermal interactions of quinones with polynuclear aromatics which lead to increased thermal reactivity and consequently an increased carbon yield from the aromatic hydrocarbons.

---

Manuscript released by the authors July 1963 for publication as an ASD Technical Documentary Report.

## 2. CHEMICAL STRUCTURE AND GRAPHITIZATION

The effects of raw material composition on graphitic quality may be illustrated by comparing synthetic graphites obtained from pure aromatic compounds of varying structure. Such a comparison is shown in Table 1 for a variety of aromatic compounds. The compounds included may be considered as prototypes of the organic species commonly present in the more complex raw materials commercially utilized in carbon and graphite production.

The compounds listed were converted to coke and graphite in three conventional stages. In the first step, they are thermally treated to 450°C to produce a raw coke. In the second step, the raw cokes are calcined to 1000°C and in the final step, the cokes are graphitized by heating to a temperature of 3000°C. The semilattice spacing obtained from the position of the 002 graphite peak has been selected as a criterion of graphiticity. These peak positions have been determined by standard X-ray diffractometer techniques for all but compounds (2), (3) and (18), the latter having been measured by X-ray camera methods. The compounds are listed in order of increasing graphiticity with natural graphite as the ultimate standard of comparison.

These data show the marked dependence of graphitization on molecular structure. Individual compounds are seen to range from the lattice spacing typical of natural graphite to the essentially "nongraphitizable" products at the bottom of the table.

Several gross conclusions can be made relating to structural effects and graphitization:

1. Linear fused polynuclear hydrocarbons such as benzo(a)pyrene, pentacene and anthracene derivatives yield highly graphitic materials.
2. Cyclopentadienyl ring systems associated with the fluorene type aromatic nucleus result in poorly ordered graphitic species as seen for such compounds as bifluorenyl, bifluorylidene, o-truxene, and fluorenone. Such ring systems are quite strained and could produce nonplanar condensed structures. On the other hand, cyclopentadienyl ring systems such as those found in acenaphthylene and rubicene are capable of rearrangement to yield planar ordered graphitic structures.
3. The large variations observed for the oxygenated compounds indicate that the thermal condensation sequence must be largely dependent on the specific functional sites and the reaction course.
4. Variation among even the fused polynuclear aromatic hydrocarbons indicate that such factors as planarity and steric considerations are important in determining the graphitization sequence.
5. Further chemical studies can be expected to amplify these relationships between chemical structure and graphitization.

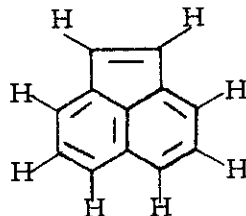
Table 1. X-Ray Comparison of Synthetic Graphite from Aromatic Compounds

Aromatic Compound	002 Lattice Spacing, A
(1) Canadian Natural Graphite	3.361
(2)* Benzo(a)pyrene	3.363
(3)* Picene	3.366
(4) Rubicene	3.366
(5) Quaterylene	3.366
(6) 7,12-Dimethylbenz(a)anthracene	3.368
(7) Acenaphthylene	3.370
(8) 9,10-Dimethylanthracene	3.373
(9) Dibenzo(a,1)pentacene	3.376
(10) 5,6,11,12-Tetraphenylnaphthacene	3.378
(11) Pentacene	3.378
(12) Decacyclene	3.378
(13) 1,7-Naphthalenediol	3.378
(14) Purpurin	3.380
(15) 9,9'-Bianthryl	3.381
(16) Naphthacene	3.383
(17) 1,4-Naphthalenediol	3.383
(18)* Dibenzo(a,c)triphenylene	3.383
(19) 7H-Benz(de)anthracene-7-one	3.383
(20) 1,5-Naphthalenediol	3.386
(21) 1,6-Naphthalenediol	3.386
(22) Benzo(a)coronene	3.388
(23) Diacenaphtho(1,2-b:1',2'-d) thiophene	3.388
(24) 2,7-Naphthalenediol	3.389
(25) 9,10-Dibenzylanthracene	3.396
(26) $\sigma$ -Truxene	3.411
(27) 9-Fluorenone	3.415
(28) 9,9'-Bifluorenyl	3.415
(29) 2-Methylanthraquinone	3.420
(30) 1,4-Naphthoquinone	3.424
(31) Quinizarin	3.424
(32) Phenanthraquinone	3.426
(33) Chrysazin	3.432
(34) 9,9'-Bifluorylidene	3.448
(35) 9,10-Dibromoanthracene	3.479

\* Measured by X-ray camera method.

## 3. CARBONIZATION OF ACENAPHTHYLENE

### 3.1. General Properties of Acenaphthylene (C<sub>12</sub>H<sub>8</sub>)



Acenaphthylene

Acenaphthylene, a yellow solid hydrocarbon, m.p. 92-93°C, is readily obtained by dehydrogenation of the hydrocarbon acenaphthene. The latter material is a common constituent of coal and petroleum tars.

Acenaphthylene is quite thermally reactive, giving rise to a 41 per cent carbon yield in an atmospheric system under normal coking conditions. This carbon, on further thermal treatment, undergoes conversion to a highly graphitic product (see Table 1). The pyrolysis of this hydrocarbon has been studied briefly by Dziewonski<sup>(2)</sup>. A review of this material may be found in an earlier report<sup>(1)</sup>.

### 3.2. Differential Thermal Analysis (DTA)

Shown in Figure 1 is a DTA thermogram for acenaphthylene. The general features of this thermogram including the melting, polymerization and depolymerization behavior (endotherm, exotherm, endotherm) have been discussed previously<sup>(1)</sup>.

### 3.3. Thermogravimetric Analysis (TGA)

Also shown in Figure 1 is a thermogravimetric analysis thermogram for acenaphthylene. The TGA behavior is consistent with that observed from the DTA. A minor weight loss occurs prior to polymerization, whereas a major weight loss is found to occur during the depolymerization endotherm at ~ 400°C.

### 3.4. Volatile Products of Acenaphthylene Pyrolysis

Summarized in Table 2 are the major volatile products obtained from the pyrolysis of acenaphthylene as identified by vapor phase chromatographic techniques.

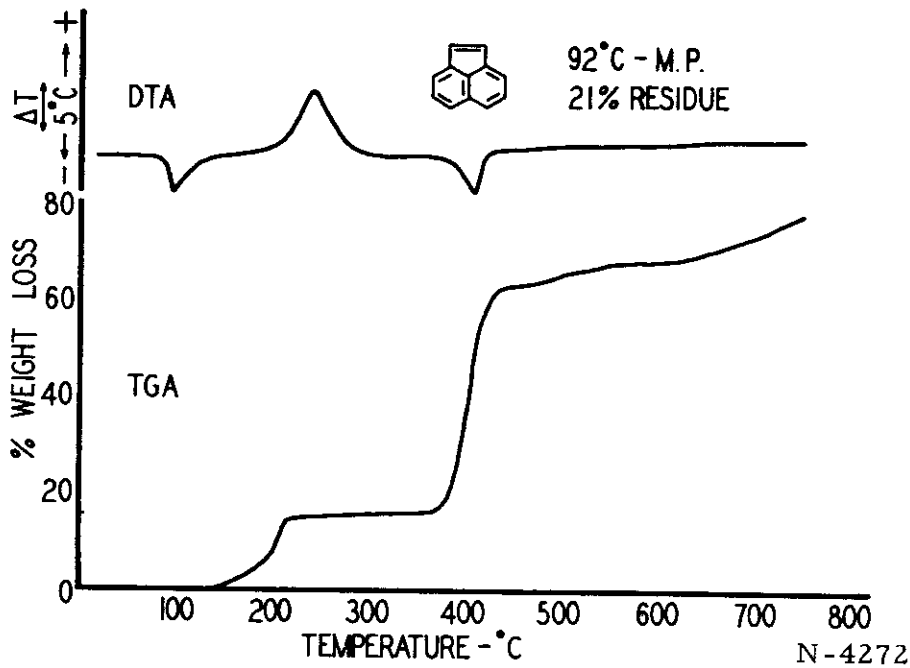
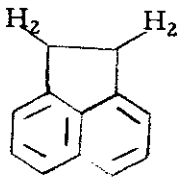


Figure 1. DTA and TGA Thermograms of Acenaphthylene

Table 2. Major Volatiles from Thermal Reaction of Acenaphthylene, 25 - 600°C

Product	Per Cent Yield
 (Acenaphthene)	~ 50
H <sub>2</sub>	~ 1.0
CH <sub>4</sub>	~ 1.0
C <sub>2</sub> H <sub>6</sub>	~ 0.2

At low temperatures the major product is the hydrogenated derivative acenaphthene; at higher temperatures significant amounts of hydrogen, methane and ethane are formed.

### 3.5. Pyrolytic Studies on Acenaphthylene

Thermal residues have been prepared at various temperature intervals and examined chemically in order to explain the pyrolytic transformations for acenaphthylene. Table 3 lists the properties of these residues; the pyrolysis temperature, percentage yield, description of residue, melting characteristics, molecular weight in benzene, per cent carbon, per cent hydrogen and atomic C/H ratio.

From these data, one may see that abrupt regions of change occur between 310° and 335°C and between 400° and 450°C. The molecular weight data show that the polymer initially formed at 185°C undergoes depolymerization at about 310°C with no apparent change in atomic carbon/hydrogen ratio and essentially no appreciable weight loss.

Pyrolysis begins above 310°C where major weight losses and increases in the atomic C/H ratio become evident. Between 310° and 400°C, the residues are black and plastic and increase in atomic C/H ratio. These residues have been found to possess the essential properties of a binder pitch and have been discussed in another report<sup>(3)</sup>.

At 450°C the essential carbonization has progressed to yield an infusible coke-like residue. Above this temperature rapid dehydrogenation ensues.

### 3.6. Ultraviolet Spectra of Acenaphthylene Thermal Residues

Shown in Figure 2 are a series of UV curves for selected acenaphthylene residues reported in Table 3. At 185°C, a decrease in long wavelength absorption is apparent. At 310°C, distinct new structural bands in the UV and visible regions are evident. Above 335°C, the materials show broad uncharacteristic spectra typical of complex aromatic mixtures such as coal tar pitch.

### 3.7. Infrared Spectra of Acenaphthylene Thermal Residues

Infrared spectral curves obtained for acenaphthylene residues in solid KBr disks are presented in Figure 3. Of major interest is the appearance of the aliphatic C-H bands in the 3.5 $\mu$  region. Additional major changes in the 10 $\mu$  to 14 $\mu$  aromatic substitution regions are evident.

### 3.8. Carbonization Mechanism of Acenaphthylene

From the data included herein and that provided from independent electron spin resonance studies<sup>(4)</sup> and low-angle X-ray measurements<sup>(5)</sup>, the following mechanistic sequence for the carbonization of acenaphthylene can be proposed.

#### 3.8.1. Polymerization

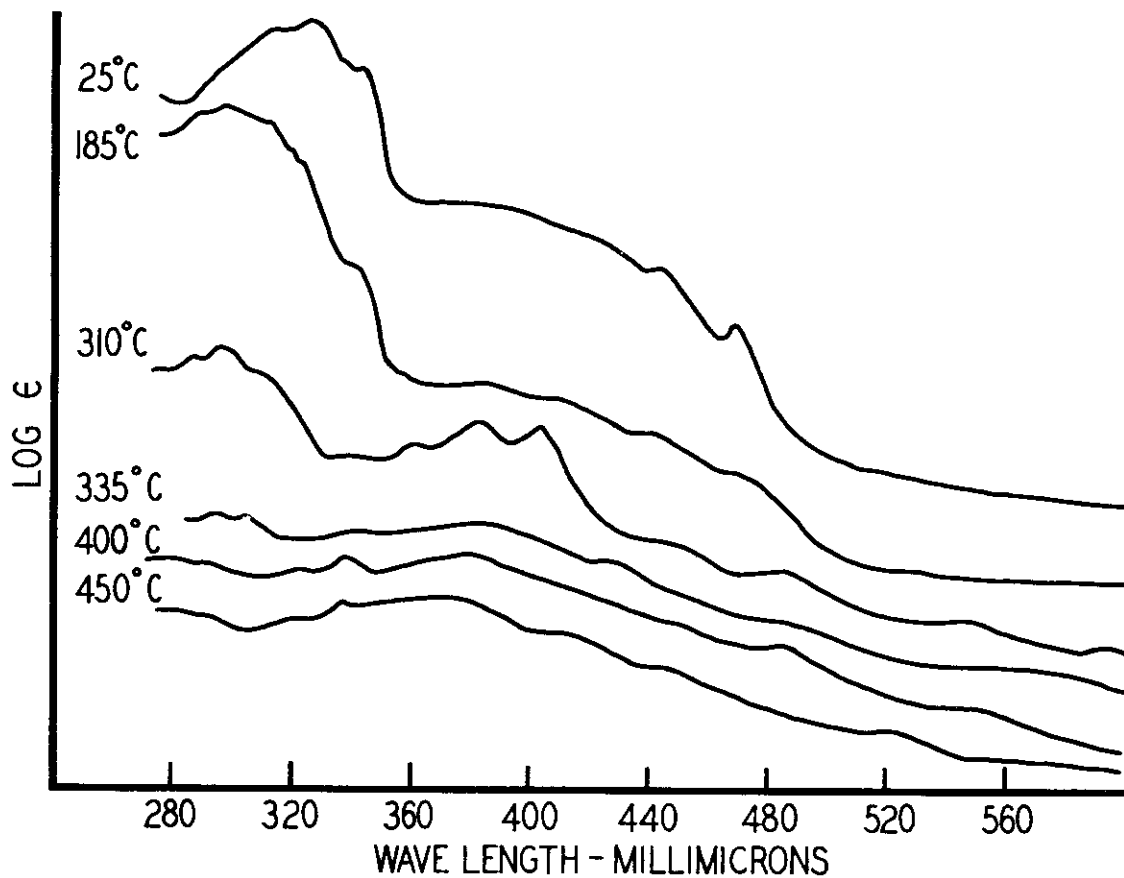
Initially at about 185°C, acenaphthylene undergoes a vinyl polymerization leading to predominantly saturated chain polymer units.



Table 3. Properties of Acenaphthylene Heat-Treated Series

Temperature °C	Yield Per Cent	Description	Melting Char. °C	Mol. Wt. in Benzene	Per Cent C	Per Cent H	Atomic Ratio C/H
25	100.0	Yellow Cryst.	92.0	152.0	94.70	5.30	1.50
185	97.9	Yellow-Orange Cryst.	250 d	1112.0	94.49	5.15	1.54
275	99.4	Orange Cryst.	249 d	1731.0	94.49	5.21	1.52
310	98.4	Brown Cryst.	261 d	733.1	94.43	5.22	1.52
335	53.1	Black-Fusible	190	501.0	95.50	4.30	1.86
350	46.8	" "	196	495.3	95.58	4.05	1.98
375	46.3	" "	192	514.7	95.85	3.95	2.02
400	45.9	" "	190	619.2	96.25	3.88	2.08
450	44.8	Black-Infusible	---	939.3	96.45	3.64	2.22
500	43.6	" "	---	Insol.	96.46	3.31	2.45
600	43.6	" "	---	"	96.72	2.66	3.05
700	42.8	" "	---	"	98.39	1.70	4.85
800	42.2	" "	---	"	99.39	0.88	4.51
1000	41.9	" "	---	"	99.96	0.23	36.0

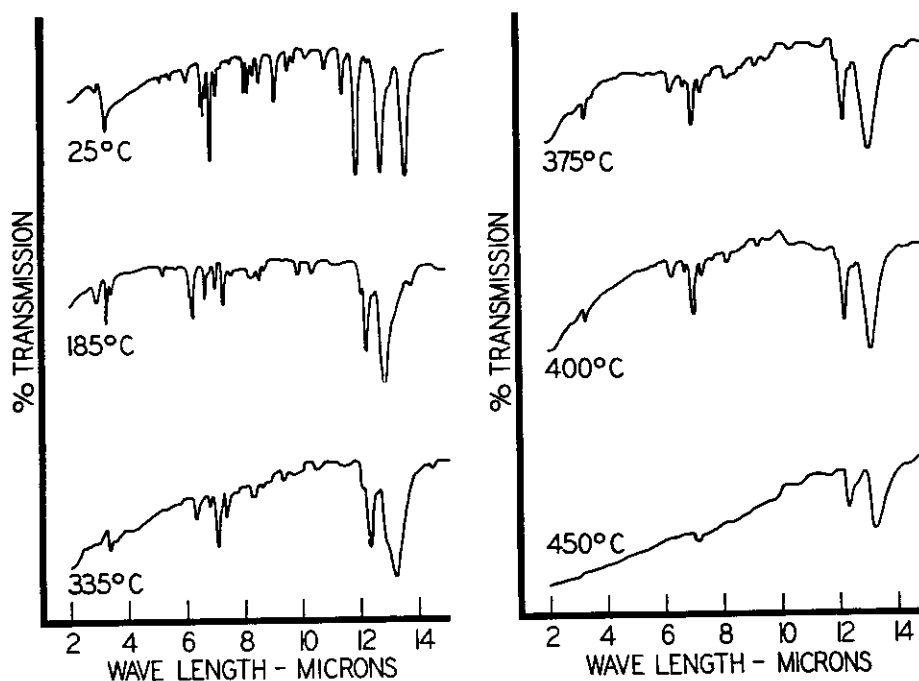
U.V. SPECTRA OF HEAT TREATED ACENAPHTHYLENE



N-4273

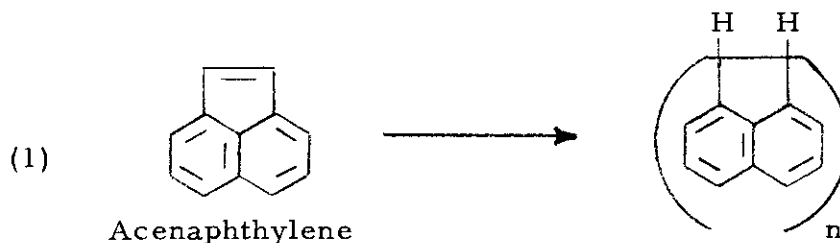
Figure 2. UV Spectra of Heat-Treated Acenaphthylene

I.R. SPECTRA OF HEAT TREATED ACENAPHTHYLENE



N-4274

Figure 3. IR Spectra of Heat-Treated Acenaphthylene

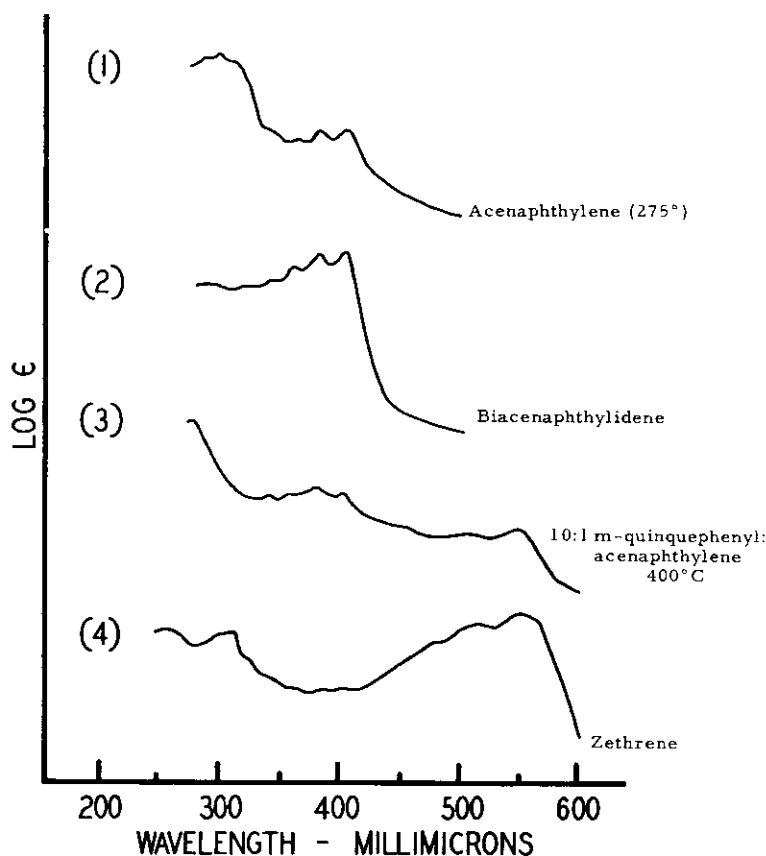


Weight average molecular weight data indicate higher polymer units than those based on the number average molecular weights in Table 3<sup>(5)</sup>. Additionally, X-ray studies indicate a helical structure for the polymer with about 3 to 5 monomer units per turn. The naphthalenic rings point outward from the axis of the helix and the polymeric CH-CH sequence is in transorientation<sup>(5)</sup>.

3.8.2. Polymer Unsaturation

The next stage in the acenaphthylene thermal transformation occurs above 250°C, whereupon the solid polymer begins to redden. Significant changes appear in the UV spectrum with bands developing at 345, 362, 380, and 403 mμ.

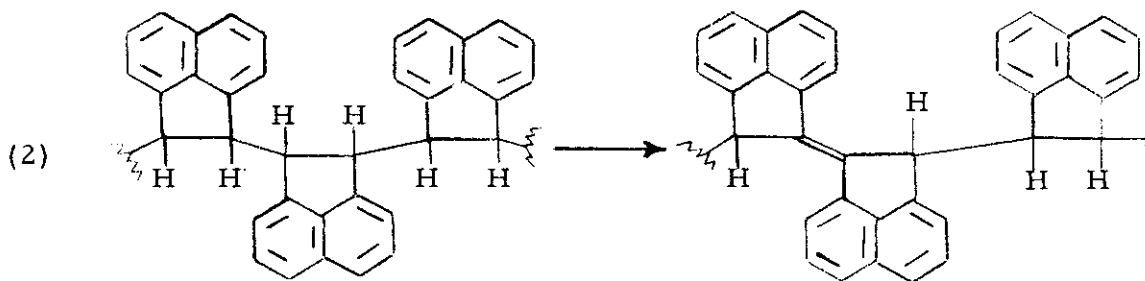
A comparison of this spectrum with that of the unsaturated dimer, biacenaphthylidene, in Figure 4, shows that the same UV pattern is obtained for both materials. No changes in the infrared spectra of the acenaphthylene polymers are apparent.



N-4275

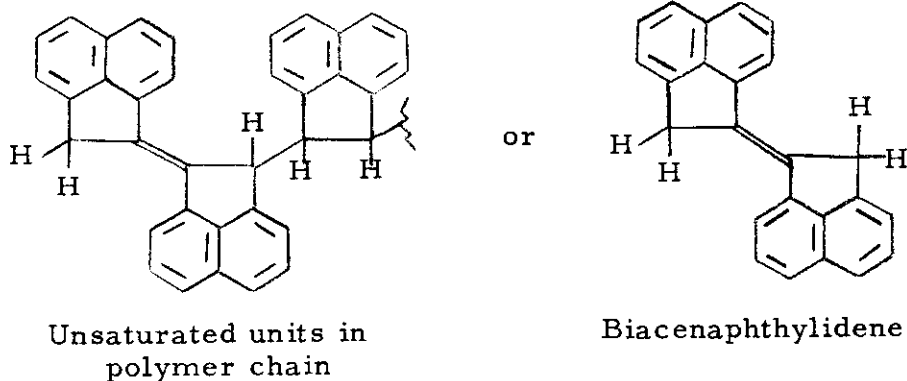
Figure 4. UV Spectra of Acenaphthylene Pyrolysis Products

These results indicate the thermal formation of unsaturated linkage between acenaphthene units in the polymer.



# Contraails

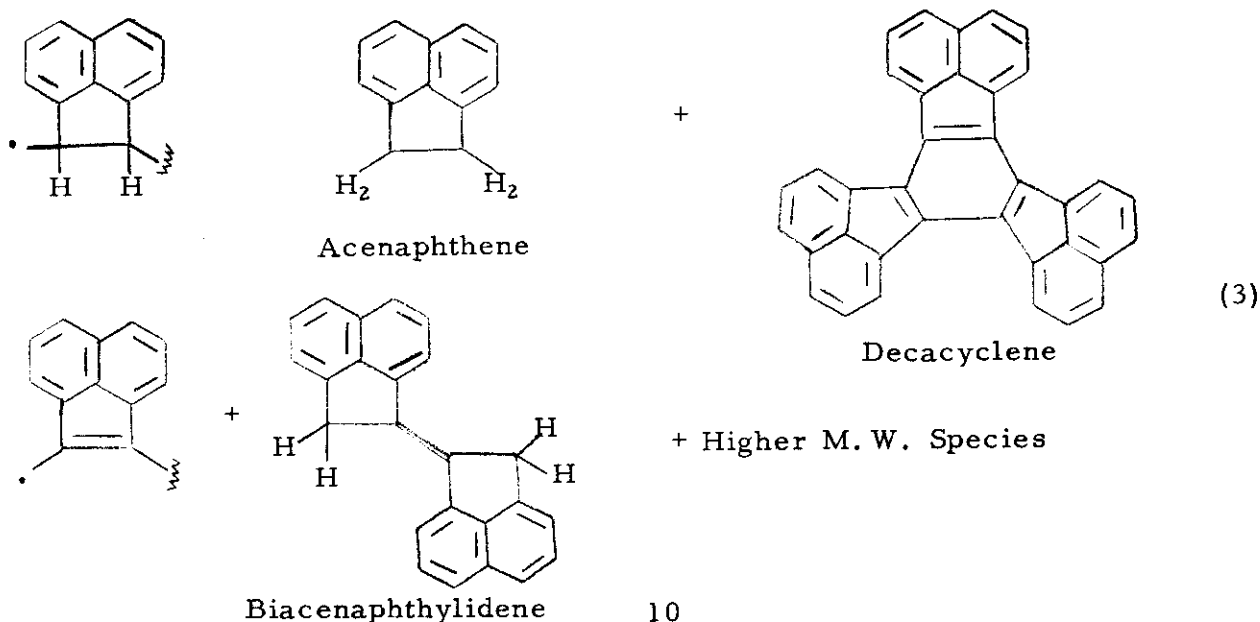
Since there is no evidence for direct dehydrogenation in the system at this stage, it is more likely that these unsaturations are accomplished by initial carbon-carbon bond cleavages between five-membered ring units in the polymer and subsequent internal transfer of hydrogen to yield units of the following types:



These reactions would involve free radical intermediates. The coiled structure of the polymer would facilitate such inter-ring hydrogen transfers.

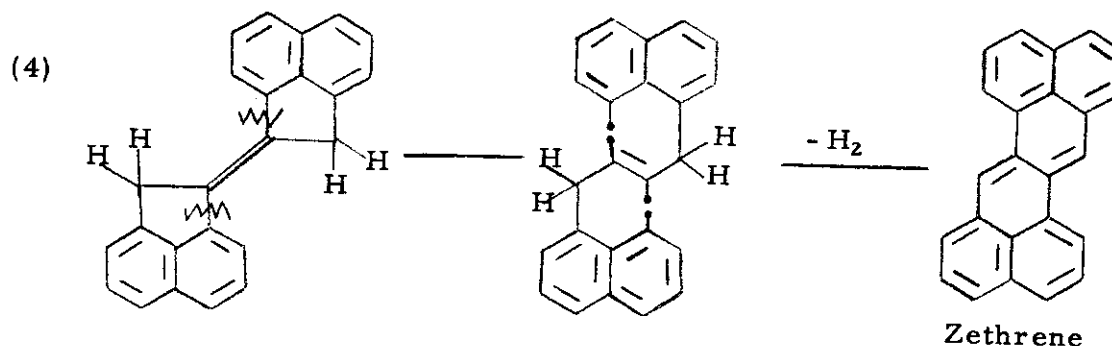
### 3.8.3. Polymer Degradation to Reactive Radicals

Above 310°C a major transformation occurs marked by the complete degradation of the polymer to lower molecular weight free radical units. These radicals could be of varying types, including acenaphthylene-like radicals, acenaphthene-like radicals and various combinations of these. Such radicals could undergo rapid hydrogen abstraction to form acenaphthene, recombine in the form of cyclic units such as decacyclene, or continue to form reactive dimer units and species related to the latter.



### 3.8.4. Rearrangement to Benzenoid Ring Systems

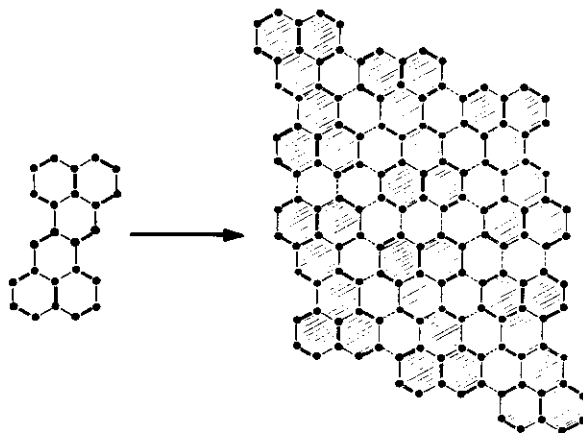
The acenaphthene is a volatile unreactive product and hence need not be considered in the carbonization sequence. The compound decacyclene has been isolated as a reaction product. X-ray studies <sup>(5)</sup> indicate that the formation of species such as decacyclene is a side reaction whereas the important carbonization sequences involve reactive intermediates of the biacenaphthylidene type. These intermediates undergo carbon-carbon bond cleavage and rearrangement to yield planar aromatic systems of the zethrene type.



Shown in Figure 4 is the UV spectrum of the hydrocarbon zethrene as obtained by Clar <sup>(6)</sup> and the comparable spectrum for the acenaphthylene pyrolysis product at 400°C in an inert diluent. The identity of the long wavelength spectral bands in addition to X-ray measurements provide good evidence for the zethrene formation.

### 3.8.5. Aromatic Planar Condensations

Zethrene would be expected from a reactivity standpoint <sup>(7)</sup> to undergo condensations, in the manner shown, producing planar contiguous aromatic ring systems. The latter would serve as prototypes for graphite.

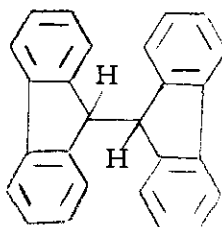


N-4276

# *Contrails*

It should be emphasized that this generalized reaction scheme presents an oversimplified picture. These thermal stages do not occur as distinct entities but as continuous overlapping transformations. Additionally, the proposed reaction intermediates must not be regarded as unique but as prototypes of similar structural species likely involved in these processes.

4. CARBONIZATION OF 9, 9'-BIFLUORENYL



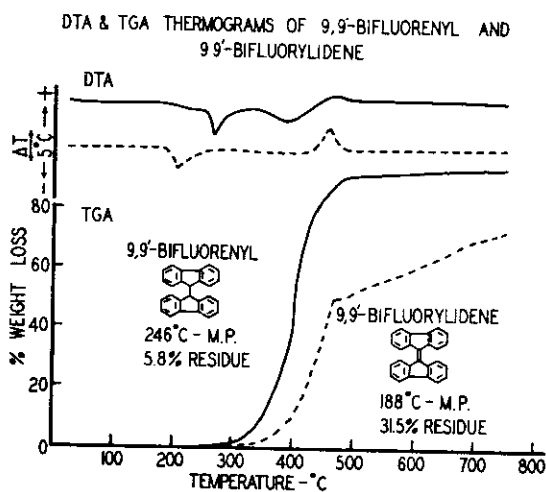
9, 9'-Bifluorenyl (C<sub>26</sub>H<sub>18</sub>)

4.1. General Properties of 9, 9'-Bifluorenyl

The aromatic hydrocarbon 9, 9'-bifluorenyl, a white solid material, m. p. 247°C, is a dimeric derivative of the hydrocarbon fluorene. The latter material is a constituent of coal tar. 9, 9'-Bifluorenyl may be carbonized to approximately 30 per cent yield. However, in contrast to acenaphthylene, it eventually yields poorly graphitic material at 3000°C. Hence bifluorenyl as a raw material for graphite lies at the opposite end of the spectrum from acenaphthylene.

4.2. Differential Thermal Analysis

Figure 5 includes DTA and TGA thermograms for both 9, 9'-bifluorenyl and the unsaturated derivative 9, 9'-bifluorylidene. Since the initial thermal sequence for bifluorenyl is a hydrogen transfer process leading to the formation of bifluorylidene, these two materials have been considered jointly.



N-4277

Figure 5. DTA and TGA Thermograms of 9, 9'-Bifluorenyl and 9, 9'-Bifluorylidene

The DTA thermogram has already been discussed in terms of this hydrogen transfer process and the subsequent exothermic transformation at ~ 450°C of the bifluorylidene moiety<sup>(1)</sup>.

#### 4.3. Thermogravimetric Analysis (TGA)

Figure 5 presents TGA curves for the compounds bifluorenyl and bifluorylidene. The very large weight loss for the bifluorenyl at about 350°C is due to distillation of fluorene formed along with the bifluorylidene at this temperature, cf. Section IVG. The rapid weight loss for bifluorylidene occurs during the exothermic reaction indicated between 400 and 450°C in the DTA thermogram.

#### 4.4. Pyrolytic Studies on 9, 9'-Bifluorenyl

Table 4 summarizes the chemical data for a series of bifluorenyl samples heat-treated at various temperatures. Compared with the acenaphthylene system, the bifluorenyl undergoes much more gradual dehydrogenation as shown by the slow increase of the atomic C/H ratio for the latter compound. Additionally, no pitch-like residue product comparable to those of acenaphthylene is formed from bifluorenyl.

Table 4. Chemical Data for 9, 9'-Bifluorenyl Heat-Treated Series

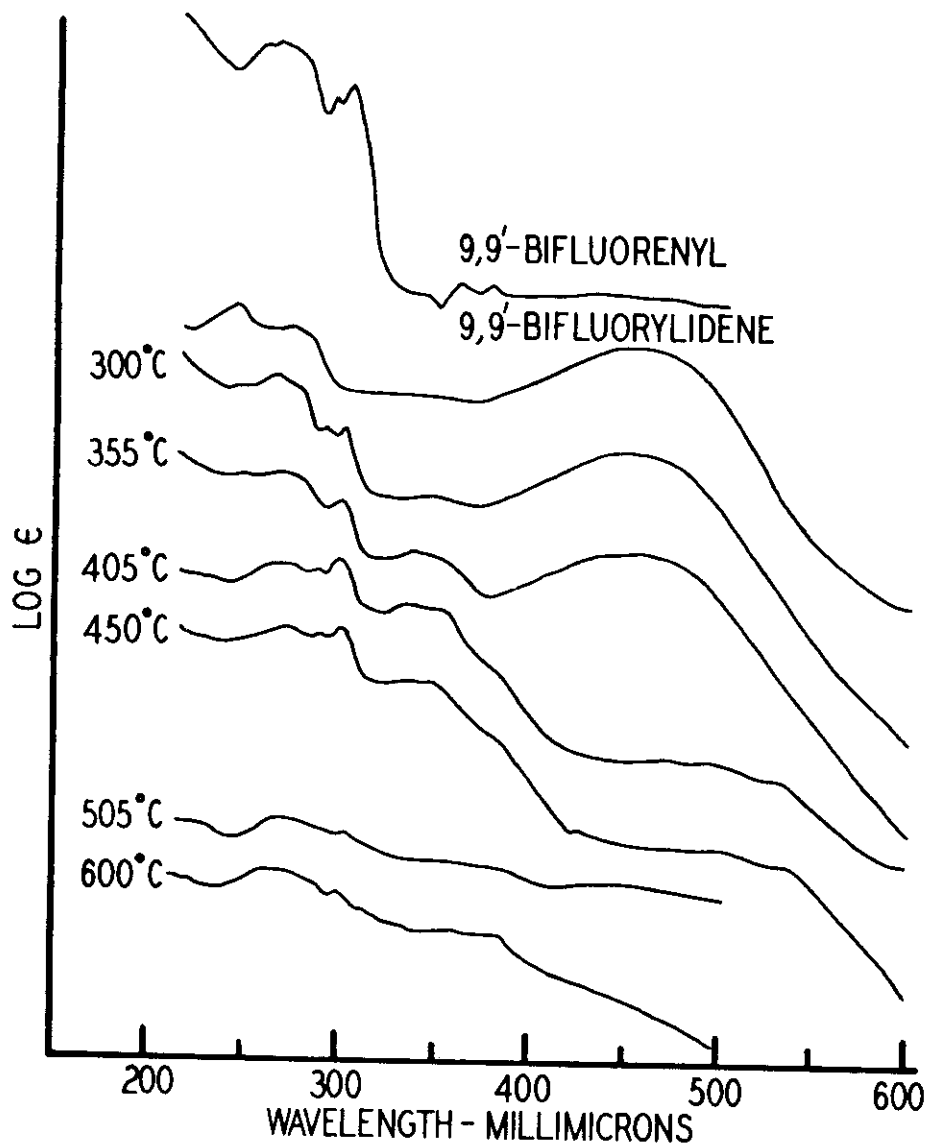
Temperature °C	Yield Per Cent	Description	Melting Char.	M. W. (C <sub>6</sub> H <sub>6</sub> )	Per Cent		Atomic C/H
					C	H	
25	100	White Solid	246°C	330	94.52	5.48	1.45
300	87.1	Orange Solid	Part 74°C Rest 142°C	288	94.06	5.33	1.48
350	63.4	Red-Orange Solid	Part 95°C Rest 162°C	410	94.71	4.94	1.61
400	41.1	Red-Brown Solid	113 - 129°C	444	94.53	4.79	1.65
450	36.1	Brown Solid	121 - 146°C	---	95.15	4.80	1.66
500	31.0	Black Solid	>360°C	---	95.67	3.73	2.15
600	28.0		Infusible	---	96.77	3.11	2.61
800	25.0		"	---	98.51	1.16	7.13
1000	24.5		"	---	-----	-----	-----

#### 4.5. Ultraviolet Absorption Spectra of Bifluorenyl Thermal Residues

Figure 6 presents a series of UV spectral curves for bifluorenyl thermal residues. Comparison with the bifluorylidene spectrum shows that bifluorylidene is formed below 300°C and then undergoes pyrolytic degradation between 350 and 405°C.



U V SPECTRA OF HEAT TREATED 9,9'-BIFLUORENYL

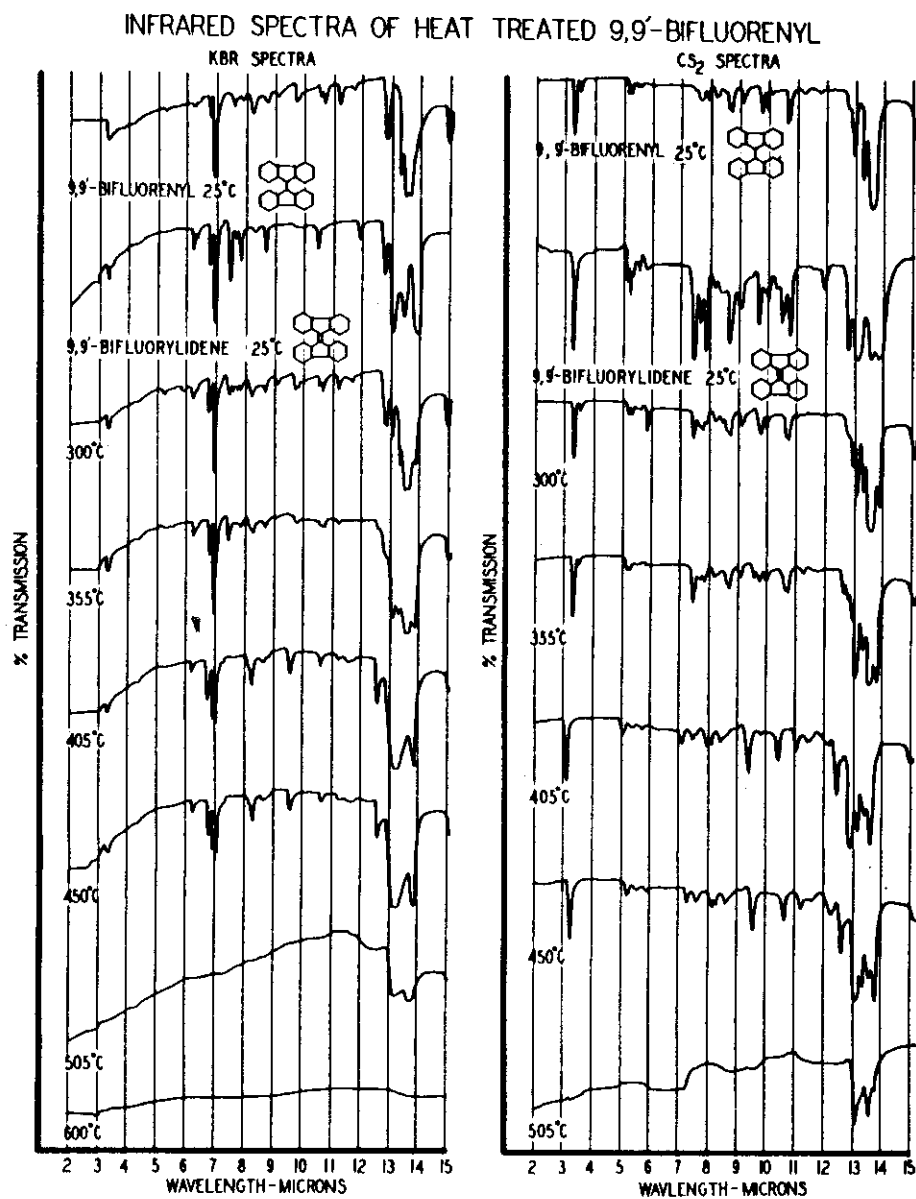


N-4278

Figure 6. UV Spectra of Heat-Treated 9,9'-Bifluorenyl

4.6. Infrared Spectra of Bifluorenyl Thermal Residues

Figure 7 includes a series of infrared spectra for bifluorenyl thermal residues obtained in KBr disks and in CS<sub>2</sub> solutions. Again comparison with the bifluorylidene spectra show the formation and breakdown of the latter product. Significant changes in the aromatic substitution region are apparent at higher temperatures.



N-4279

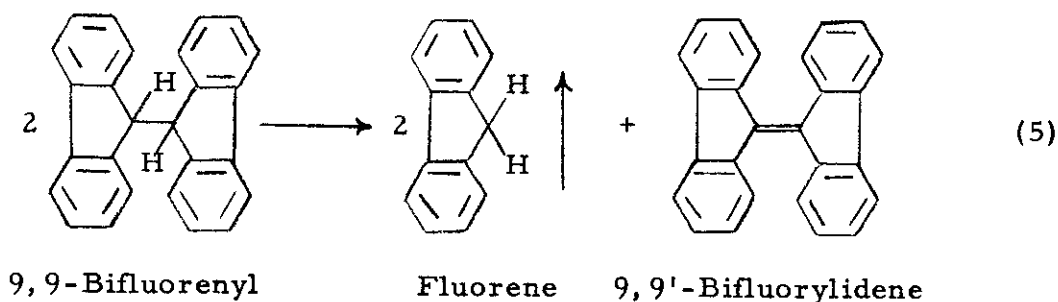
Figure 7. Infrared Spectra of Heat-Treated 9,9'-Bifluorenyl

## 4.7. Thermal Reactions for 9, 9'-Bifluorenyl

The data included herein, supplemented by separately reported ESR studies, <sup>(4)</sup> suggest the following initial thermal sequences for 9, 9'-bifluorenyl.

### 4.7.1. Dehydrogenation to Bifluorylidene

Initially, bifluorenyl proceeds through internal hydrogen transfer to form fluorene plus bifluorylidene at about 300°C.



### 4.7.2. Ring Cleavage and Recombination

The volatile thermally stable fluorene <sup>(1)</sup> is not involved in further carbonization reactions which are restricted to the bifluorylidene species. Present results indicate that these species undergo ring cleavage at the biphenyl bridge. This cleavage leads to the formation of nonplanar radical species which can combine with like radicals to form 3-dimensionally cross-linked polymers, or, by rotation and recombination, can form nonplanar benzenoid systems such as tetrabenzonaphthalene. The formation of fluorene as a by-product in this sequence provides another example of thermal hydrogen migration to active bond sites.

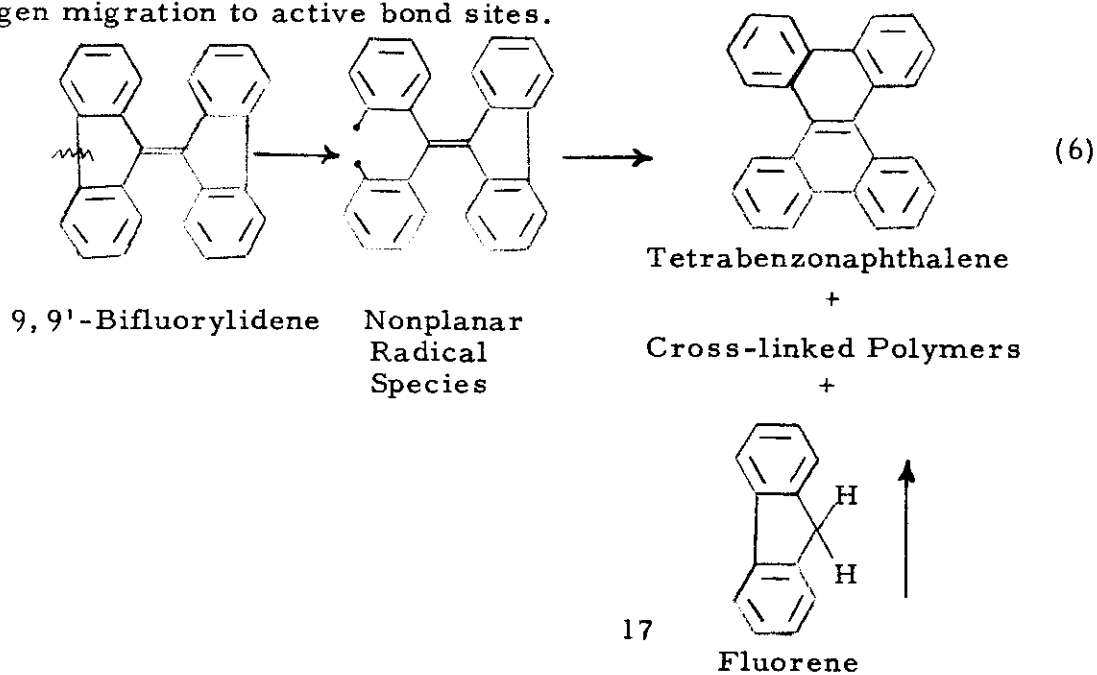
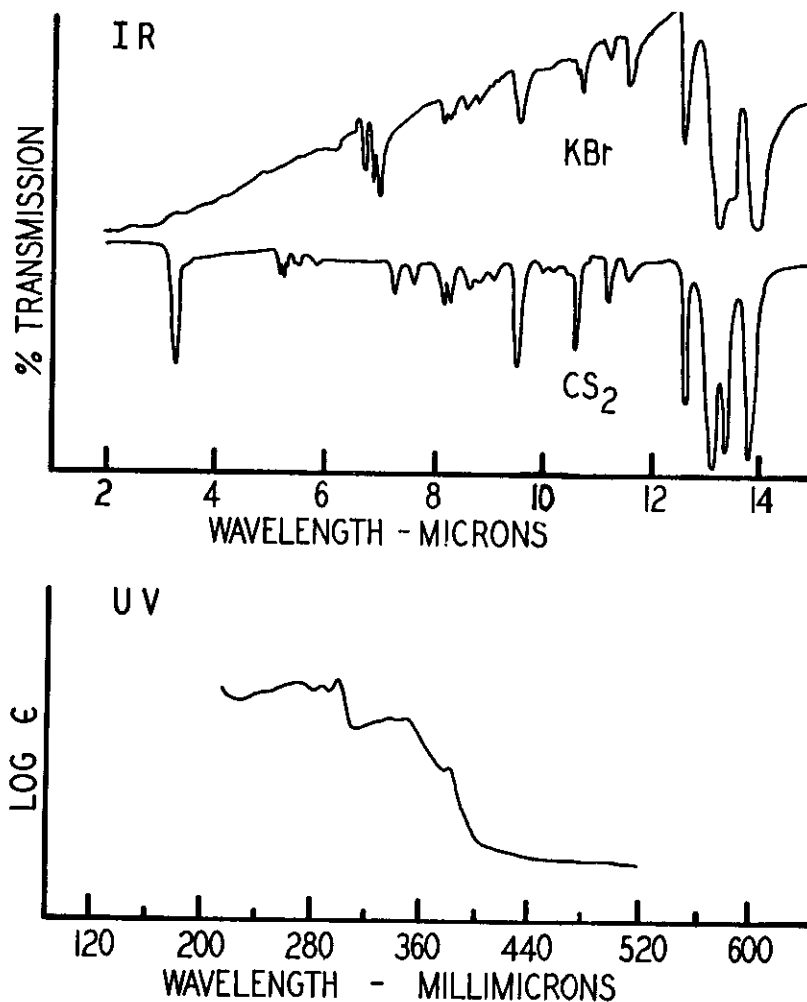


Figure 8 presents the UV and IR spectra for tetrabenzonaphthalene. Comparison with the bifluorenyl spectra in Figures 6 and 7 shows that the formation of tetrabenzonaphthalene occurs generally in the vicinity of 400°C. Rapid condensation of the radical entities appears to occur exothermically at about 450°C.



N-4288

Figure 8. Infrared and Ultraviolet Spectra of Tetrabenzonaphthalene

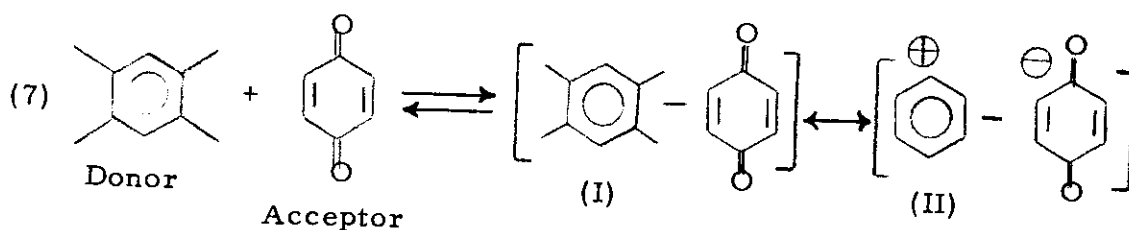
Investigations, which will attempt to explain the further stages of carbonization, are continuing. The formation of nonplanar reactive aromatic intermediates from 9, 9'-bifluorenyl appears to be a significant factor in the explanation of the poor graphitizability of the pyrolytic residues.

## 5. THE EFFECTS OF QUINONE ADDITIVES ON THE CARBONIZATION OF POLYNUCLEAR AROMATICS

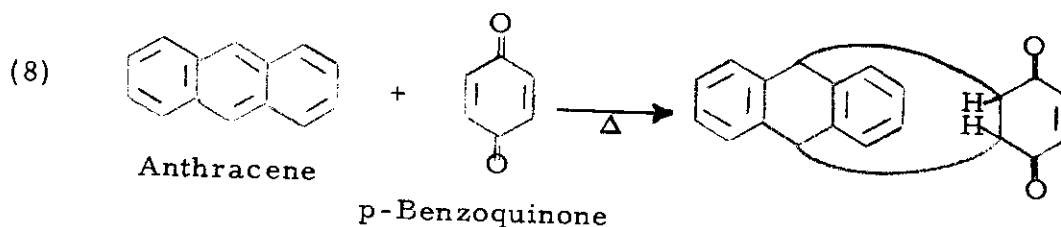
### 5.1. Mechanisms of Quinone-Aromatic Interactions

Quinones are known to interact with aromatic hydrocarbons in several ways:

1. Charge-transfer complex formation -- Mülliken<sup>(8)</sup> has discussed the theory of charge transfer formation between various kinds of molecular donors and molecular acceptors. Briegleb and Czekalla<sup>(9)</sup> have demonstrated such interactions spectrophotometrically between polynuclear aromatics and quinones. The quinones act as electron acceptors and the aromatics as electron donors. This interaction as illustrated in Equation (7) involves the reversible formation by partial electron transfer of a complex which may be considered a resonance hybrid of two structures: (I) a loose association of donor and acceptor and (II) a completely electron-transferred state.

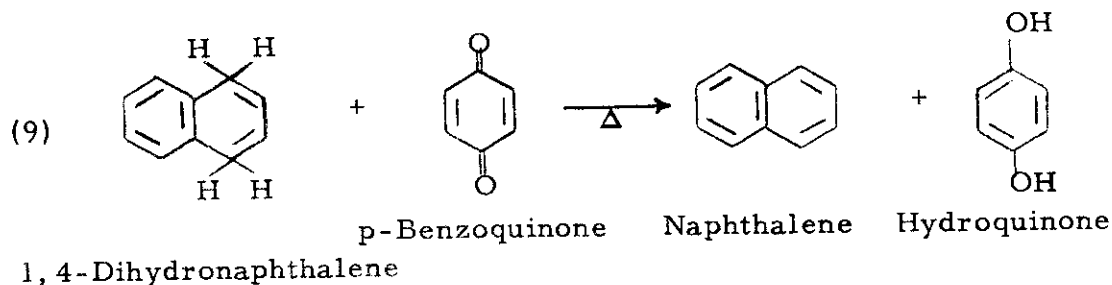


2. Diels-Alder Addition -- Quinones are known to form Diels-Alder adducts with certain types of polynuclear aromatics as illustrated by the reaction between p-benzoquinone and anthracene<sup>(10)</sup>. This reaction can result in the formation of higher molecular weight polymeric adducts.



3. Dehydrogenation -- Quinones have been found to act as dehydrogenating agents to hydrogenated aromatics. The conversion of 1,4-dihydronaphthalene to naphthalene by the action of p-benzoquinone is illustrative of this reaction<sup>(11)</sup>.

# Contrails



All three processes should have the effect of increasing the reactivity of aromatic hydrocarbons towards carbonization. Charge transfer complexing and addition reactions would tend to stabilize the aromatic structure from early volatilization, whereas the dehydrogenation action should convert hydroaromatic systems to more thermally reactive aromatic entities.

The results which follow demonstrate the general effect of quinones in increasing the extent of carbonization of some polycyclic aromatic hydrocarbons and coal tar pitches.

## 5.2. Experimental

Coking of the pure compounds and mixtures was performed in Pyrex beakers which were covered with watch glasses and inserted into protective triple saggars. The heating schedule employed was 60°C/hr from 25°C to 390°C, with a 10-hour hold at 390°C, followed by a 60°C/hr heat-treatment to 450°C, with a 3-hour hold. The beakers were weighed before and after heating to ascertain the 450°C coking values.

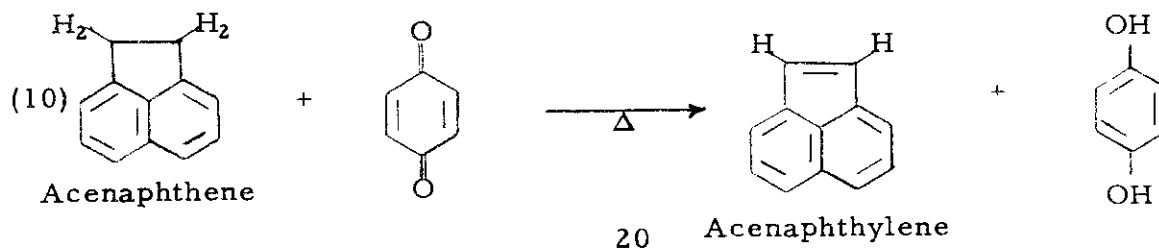
All chemicals were obtained from commercial supply houses and used without further purification.

UV spectra for the ionization potential calculations were obtained with a Beckman-DK Spectrophotometer in a manner described previously<sup>(1)</sup>.

## 5.3. Results and Discussion

### 5.3.1. Thermal Interactions of Quinones with the Aromatic Hydrocarbon Acenaphthene

The efficacy of various quinones as dehydrogenating agents as a means of increasing carbonization may be demonstrated by use of the hydroaromatic compound acenaphthene as a hydrogen donor. Thermal interaction with a quinone would be expected to proceed via Equation (10).



The hydrocarbon acenaphthylene formed by this reaction has been shown to be highly reactive to carbonization as contrasted to the inert acenaphthene. Hence, the addition of a quinone to acenaphthene should induce carbonization.

Table 5 shows the effects of a variety of quinone additives on the coking value of acenaphthene. The individual coking values of the quinones, given in the second column, are seen to vary from 0 to 87 per cent. In the third column are the coking values of 1:1 mixtures of the respective quinone and acenaphthene. Since the latter compound has a zero coking value, the expected coking values would be half the figures in column 2. Column 4 lists the increases in coking value over that based on the quinone alone. Finally, the last column presents the oxidation-reduction potentials of each quinone.

It is evident that each quinone induces some carbonization of the acenaphthene moiety. The effects observed range from 2.0 for 9,10-phenanthraquinone to 49 per cent for 2,3-dichloro-1,4-naphthoquinone, the most active quinone additive.

Table 5. Effect of Quinones on the Coking Values of Acenaphthene

Quinone	C. V. of Quinone Per Cent	C. V. 1:1 Acenaphthene Quinone Mixture Per Cent	$\Delta$ C. V. Per Cent	Quinone Oxidation Potential
(1) None	----	0.0	0.0	-----
(2) 9,10-Phenanthraquinone	87.2	45.6	2.0	0.458
(3) 1,4-Naphthoquinone	0.1	20.1	20.0	0.156
(4) 9,10-Anthraquinone	80.5	50.6	10.3	0.484
(5) Chloranil	3.0	30.5	29.0	0.703
(6) 2,6-Dichloro-p-benzoquinone	34.5	46.4	29.1	0.749
(7) 2-Chloro-anthraquinone	17.1	47.7	39.1	0.203
(8) p-Benzoquinone	5.4	44.2	41.5	0.711
(9) 2,3-Dichloro-1,4-naphthoquinone	23.4	60.7	49.0	0.500

There is no obvious relationship between the oxidation-reduction potential and the quinone action as might be anticipated for a simple dehydrogenation sequence. It is apparent that all of the halogenated quinones are quite reactive, regardless of their oxidation potential.

These results imply that not only dehydrogenation effects are involved. The reciprocal action of the acenaphthene on the carbonization of the quinone is undoubtedly significant. Furthermore, stabilization through charge transfer formation is believed to be important. It should be mentioned that the most reactive quinone, 2,3-dichloro-1,4-naphthoquinone, complexes with acenaphthene in the solid phase at room temperature.

5.3.2. Thermal Interaction of p-Benzoquinone with Polynuclear Aromatic Hydrocarbons

The generality of the quinone-aromatic interaction may be demonstrated by the effect of a single active quinone, p-benzoquinone, on the carbonization of a variety of aromatic hydrocarbons. Such a comparison is shown in Table 6 for 28 aromatic hydrocarbons.

Table 6. Coking Interaction of p-Benzoquinone\* with Aromatic Hydrocarbons

Aromatic	Aromatic C. V. 450°C Per Cent	C. V. 1:1 Aromatic p-B.Q. Mixt. Per Cent	Δ C. V. Per Cent	I. P. (e. v.)
(1) Biphenyl	0.0	1.5	0.0	8.69
(2) Triphenylene	0.0	1.7	0.0	8.14
(3) Naphthalene	0.0	1.3	0.0	8.12
(4) Phenanthrene	0.0	1.0	0.0	8.03
(5) 2-Methylphenanthrene	0.0	3.9	1.2	8.01
(6) Triphenylethylene	3.1	2.5	0.0	7.93
(7) Tetraphenylethylene	3.4	1.0	0.0	7.77
(8) Chrysene	0.0	12.6	9.9	7.75
(9) Pyrene	0.0	5.7	3.0	7.56
(10) 2-Methylpyrene	0.0	7.0	4.3	7.54
(11) Acenaphthylene	41.8	58.6	35.0	7.53
(12) Trans-stilbene	0.0	5.9	3.2	----
(13) Coronene	0.5	18.2	15.1	7.50
(14) Benz [e] acephenanthrylene	0.0	2.5	0.0	7.42
(15) Dibenz - [a, h] -anthracene	1.0	20.2	17.0	7.42
(16) Benz - [a] -anthracene	0.0	25.7	23.0	7.35
(17) Benzo [a] pyrene	0.0	13.8	11.1	7.31
(18) Dibenzo [a, e] pyrene	1.8	0.6	0.0	7.23
(19) Anthracene	0.0	35.5	32.8	7.22
(20) 7, 12-Dimethylbenz [a] anthracene	4.2	23.2	18.4	7.18
(21) Dibenzo [h, rst] pentaphene	6.5	33.5	27.6	7.18
(22) Benzo [g, h, i] perylene	1.1	6.3	3.1	7.17
(23) 9, 10-Dimethylantracene	2.6	33.9	30.0	7.06
(24) Perylene	0.0	43.7	41.0	6.84
(25) 9, 9' -Bifluorenyl	58.6	33.3	1.3	6.70
(26) Naphthacene	40.0	69.1	46.4	6.64
(27) Dibenzo [a, l] pentacene	40.2	43.4	20.6	6.40
(28) Pentacene	49.8	60.7	33.1	6.23

\* Coking value of p-benzoquinone alone = 5.4 per cent.



The second column presents the 450°C coking values of the individual aromatic hydrocarbons. The majority of these materials are found to be thermally unreactive under the conditions of measurement. Column 3 lists the coking values for a 1:1 mixture of the aromatic and p-benzoquinone. Column 4 shows the increase in carbon formation over that predicted on a straight additive noninteracting basis. Column 5 lists the ionization potential reactivity parameters for the individual hydrocarbons derived spectroscopically by a previously described method (1).

The enhanced coking value through quinone interaction is quite general for the more reactive aromatics (low I. P.). Virtually no effects are observed for aromatics with I. P. > 7.75. Charge transfer complexing is thought to be a significant factor since complex stability is related to aromatic reactivity (12); hence, the compounds of high I. P. are not expected to undergo extensive complex formation. Volatility is not believed to be important since the quinone-aromatic reactions have been found to occur generally in the vicinity of 200°C, (13) which is below the boiling point of these materials.

For the remaining reactive hydrocarbons, only a crude relationship between  $\Delta C. V.$  and I. P. is apparent. This result is not surprising since each of the 3 mechanisms discussed in Section 5.3.1. can be operative.

### 5.3.3. Thermal Interaction of p-Benzoquinone with Hydroaromatic Compounds

Even more dramatic effects are observed for the reaction of p-benzoquinone with hydrogenated aromatic systems. Such data are shown in Table 7 for eight aromatic hydrocarbons containing aliphatic hydrogens in the ring. Extreme coking value enhancements ( $\Delta C. V.$ ) are evident for nearly all the listed compounds. These reactivities bear no relationship to the I. P. reactivity parameters listed in the last column. The dehydrogenation sequence (Equation 9) is believed to be operative in these systems.

Table 7 also presents the coking value of a 1:1 mixture of p-benzoquinone and a nitrogen heterocyclic, acridine. The  $\Delta C. V.$  of 51.5 per cent is among the highest observed and is second only to that of chrysofluorene.

### 5.3.4. Effects of Quinones on the Coking Values of Coal Tar Pitches

It is of interest to explore the effects of quinone additives on the coking values of coal tar pitches which to a great extent include mixtures of aromatic, hydroaromatic and heterocyclic species. Such effects could be utilized for improving binder systems.

Experiments have been completed for pitch-quinone mixtures employing 4 different quinones and 3 representative commercial coal tar pitches of varying physical properties. The individual coking values of these materials are given in Table 8.

Table 7. Coking Interactions of p-Benzoquinone with Aromatic Hydrocarbons Containing Aliphatic Hydrogens in the Ring

Aromatic	Per Cent			I. P. (e. v.)
	Aromatic C. V. 450°C	C. V. 1:1 Aromatic p-B. Q. Mixt.	Δ C. V.	
(1) Fluorene	0.0	42.5	39.8	8.46
(2) 9, 10-Dihydroanthracene	0.0	34.3	31.6	8.32
(3) Acenaphthene	0.0	44.1	41.4	7.72
(4) 5, 12-Dihydronaphthacene	7.3	41.8	35.4	7.71
(5) Chrysofluorene	0.0	56.8	54.1	7.52
(6) 9, 9'-Bifluorenyl	21.4	41.1	27.7	7.31
(7) 14H-Acenaph [1, 2-j] indeno [1, 2-ℓ] fluoranthene	59.4	40.9	8.5	7.03
(8) 4, 5, 9, 10-Tetrahydroprene	0.0	3.7	1.0	----
-----				
(9) Acridine (Heterocyclic)	2.0	55.2	51.5	----

Table 8. Coking Values of Pure Materials Employed in Quinone Pitch Study

Material	Coking Value at 450°C Per Cent
1. 9, 10-Anthraquinone	0.1
2. 1, 4 Naphthoquinone	80.5
3. Chloranil	3.0
4. p-Benzoquinone	5.4
5. 175° Pitch	81.1
6. 30 Medium Pitch	63.1
7. 240 Tar	27.0

Summarized in Table 9 are the results of coking experiments using all combinations of the four quinones in 25 per cent proportions with 75 per cent of the three pitches. In every case the quinone shows a pronounced effect toward increasing the coking values of the coal tar pitch. The most active quinones

# Contrails

(highest  $\Delta$  C. V. ) are p-benzoquinone and chloranil; the results reported in the previous section on pure compounds are consistent with those revealed here. From a practical standpoint, however, the 1,4-naphthoquinone might be the most desirable additive due to its high individual coking value. The most effective quinone action occurs in all cases with the lowest melting and lowest coking material, the 240 tar. The least effective action is with the high melting 175°C pitch.

Table 9. Effects of Quinone Additives on Coking Values of Coal Tar Pitches

Mixture	Actual C. V. 450°C Per Cent	Calculated C. V. 450°C * Per Cent	$\Delta$ C. V. Per Cent
1. 25% chloranil + 75% 175° pitch	77.8	61.5	16.3
2. 25% chloranil + 75% 30 medium pitch	74.5	48.0	26.5
3. 25% chloranil + 75% 240 tar	57.9	21.0	36.9
4. 25% 1,4-naphthoquinone + 75% 175° pitch	85.7	81.0	4.7
5. 25% 1,4-naphthoquinone + 75% 30 medium pitch	73.5	67.2	6.3
6. 25% 1,4-naphthoquinone + 75% 240 tar	56.4	40.4	16.0
7. 25% 9,10-anthraquinone + 75% 175° pitch	66.0	60.8	5.2
8. 25% 9,10-anthraquinone + 75% 30 medium pitch	53.9	47.1	6.8
9. 25% 9,10-anthraquinone + 75% 240 tar	37.5	20.3	17.2
10. 25% p-benzoquinone + 75% 175° pitch	79.5	62.2	17.3
11. 25% p-benzoquinone + 75% 30 medium pitch	71.0	48.7	22.3
12. 25% p-benzoquinone + 75% 240 tar	51.7	21.6	30.1

\* Calculated using the coking values of the individual components.

# *Contrails*

Quinones thus, have been shown to have a general effect on increasing the coking values of pure aromatic compounds and of coal tar pitches. The mechanisms of these actions are believed to be of three types; complex formation, addition and dehydrogenation.

6. REFERENCES

1. WADD Technical Report 61-72, Volume X, Thermal Reactivity of Aromatic Hydrocarbons, by I. C. Lewis and T. Edstrom.
2. K. Dziewonski, Chem.Ber. 53, 142 (1920) and references cited therein
3. WADD Technical Report 61-72, Volume XXXII, Studies of Binder Systems for Graphite, by T. Edstrom, I. C. Lewis, R. L. Racicot and C. F. Stout.
4. WADD Technical Report 61-72, Volume XVI, An Electron Spin Resonance Study of Thermal Reactions of Organic Compounds, by L. S. Singer and I. C. Lewis.
5. Unpublished Results by W. O. Ruland, Union Carbide European Research Associates.
6. E. Clar, K. F. Lang and H. Schulz - Kiesow, Chem. Ber. 88, 1520 (1955).
7. C. A. Carlson, C. M. Moser and M. P. Barnett, J. Chem. Soc. 3108 (1954).
8. R. S. Mulliken, J. Am. Chem. Soc. 72, 600 (1950); 74, 811 (1952).
9. G. Brieglab and J. Czekalla, Z. Elektrochem 63, 6 (1959).
10. E. Clar, Chem. Ber. 64, 1676 (1931).
11. E. A. Braude, L. M. Jackman and R. P. Linstead, J. Chem. Soc. 3548 (1954).
12. J. B. Birke and M. A. Slykin, Nature 191, 701 (1961).
13. WADD Technical Report 61-72, Supplement to Volume X, Thermal Reactivity of Aromatic Hydrocarbons, by I. C. Lewis and T. Edstrom.

# *Contrails*

# *Contrails*

# *Contrails*